EFFECTS OF FIRE-DAMAGE ON THE NONLINEAR RESPONSE OF R.C. BASE-ISOLATED BUILDINGS UNDER NEAR-FAULT EARTHQUAKES

F. Mazza[(1)], F. Alesina[(2)]

[(1)] *Researcher, Dipartimento di Ingegneria Civile, Università della Calabria, Rende (Cosenza), Italy, fabio.mazza@unical.it*
[(2)] *Ph.D., Dipartimento di Ingegneria Civile, Università della Calabria, Rende (Cosenza), Italy, fabioalesina@yahoo.it*

Abstract

The increase in the deformability of a fire-damaged base-isolated building may lead to an amplification in the structural response under the long-duration horizontal pulses of near-fault earthquakes. Moreover, high values of the peak acceleration ratio, defined as the ratio between the peak value of the vertical acceleration and the analogous value of the horizontal acceleration, can become critical once the strength level of a fire-weakened base-isolated structure is reduced. To study the nonlinear seismic response following fire, a numerical investigation is carried out on six-storey r.c. base-isolated structures, composed of a basement and five storeys above the ground level, designed in line with the Italian seismic code. The base-isolation system is constituted of High-Damping-Laminated-Rubber Bearings (HDLRBs). Different values of fire resistance and opening factor representing the amount of ventilation are considered, in line with the parametric temperature-time fire curve proposed by Eurocode 1. Three fire scenarios are examined, with the fire compartment confined to the area of the base-isolated level (i.e. F0) and first (i.e. F1) and fifth (i.e. F5) levels of the superstructure. A numerical investigation is carried out by means of thermal-mechanical mapping analysis, with reduced mechanical properties of both r.c. cross-sections, in line with the 500°C isotherm method proposed by Eurocode 2, and HDLRBs, in line with a proposed 200°C isotherm method. A nonlinear incremental dynamic analysis considers the horizontal and vertical components of near-fault earthquakes. Plastic conditions are assessed at the potential critical sections of the beams (i.e. end sections of the sub-elements in which a beam is discretized) and columns (i.e. end sections). The response of a HDLRB is simulated with a viscoelastic model with variable stiffness properties in the horizontal and vertical directions, depending on the axial force and lateral deformation.

Keywords: Base-isolated framed structures; Fire damaged r.c. members; Fire damaged HDLRBs; Near-fault earthquakes.

1. Introduction

Elastomeric bearings (e.g. the High-Damping-Laminated-Rubber Bearings, HDLRBs) are a very popular and effective base-isolation system for the seismic protection of new constructions, even if structural damage is expected in the case of base-isolated structures subjected to the horizontal and vertical components of near-fault earthquakes [1]. In particular, fling-step and forward-directivity effects in near-fault areas can produce one- and two-sided long-duration (horizontal) velocity pulses, respectively, with and without permanent ground displacement [2]. Moreover, near-fault ground motions can be characterized by high values of the peak acceleration ratio α_{PGA} [3], defined as the ratio between the peak value of the vertical acceleration (PGA_V) and the analogous value of the horizontal acceleration (PGA_H). Little is known, however, about the seismic response following fire of a reinforced concrete (r.c.) base-isolated framed structure. A significant decrease of stiffness, strength and ductility affects the r.c. members exposed to fire [4]. Thus, an amplification of the structural damage of a fire-weakened base-isolated structure subjected to near-fault ground motions is found, especially where the fire compartment is assumed [5]: i.e., at the lower levels, for long-duration (horizontal) velocity pulses due to directivity and fling-step effects; at the higher levels, for high values of the acceleration ratio α_{PGA}. On the other hand, there is a lack of knowledge in the seismic response of base-isolated structures with fire-exposed HDLRBs, in which the influence of temperatures higher than that of vulcanization between layers of rubber and steel plates reduces mechanical and geometrical properties of the base-isolation system [6, 7].

To study the nonlinear seismic response following fire, a numerical investigation is carried out on six-storey r.c. base-isolated structures, composed of a basement and five storeys above the ground level, designed in line with the Italian seismic code [8]. The base-isolation system consists of HDLRBs, inserted at the top of the columns of the basement, with different values of the ratio between vertical and horizontal stiffnesses. Both fire-protected HDLRBs, delaying the transfer of heat for a duration not less than that required for the fire resistance of the superstructure, and fire-exposed HDLRBs, in which the influence of high temperatures on the material properties is considered, are examined for the base-isolation system. Parametric temperature-time fire curves are evaluated in accordance with Eurocode 1 (EC1, [9]), with different values of the opening factor representing the amount of ventilation. Three fire scenarios are examined, assuming the fire compartment confined to the area of the base-isolated level (i.e. F0) and first (i.e. F1) and fifth (i.e. F5) levels of the superstructure. R.c. frame members and HDLRBs experience damage during fire and their response after fire is closely related to the residual load capacity. Thus, a numerical fire investigation is carried out considering a thermal-mechanical mapping analysis, with reduced mechanical properties evaluated in line with the 500°C isotherm method proposed by Eurocode 2 (EC2, [10]), for r.c. cross-sections, and a proposed 200°C isotherm method, for the layers of rubber. A nonlinear incremental dynamic analysis is carried out considering the horizontal and vertical components of nine near-fault ground motions, available in the *Pacific Earthquake Engineering Research Center database* [11].

2. Base-isolated test structures: seismic design and fire modelling

A six-storey r.c. base-isolated office building with a symmetric plan (Fig. 1a), composed of a basement and five-storey above the ground level (Fig. 1b), is considered as test structure for the numerical investigation. The length and cross-sections of the frame members are also shown in Fig. 1. The base-isolation system consists of fifteen identical HDLRBs inserted at the top of the columns of the basement. A grid of rigid beams is placed at the base of the superstructure on the HDLRBs. In order to account for the plastic deformations along the beams, each is discretized into four sub-elements of the same length and lumped masses are considered at the end, quarter-span and mid-span sections. Both fire-protected and fire-exposed HDLRBs are considered, assuming three values (i.e. 400, 800 and 2400) of the ratio α_{K0} between vertical (K_{V0}) and horizontal (K_{H0}) nominal stiffnesses of the isolation system. Three fire scenarios are also reported in Fig. 1, with the fire compartment confined to the area of the base-isolated level (i.e. basement, F0) and first (i.e. F1) and fifth (i.e. F5) floor levels of the superstructure.

The design of the base-isolated (BI) test structures is carried out in line with the Italian seismic code (NTC08, [8]) considering, besides the gravity loads, the horizontal seismic loads acting in combination with the vertical ones. Moreover, the following assumptions are made: elastic response of the superstructure (behaviour factors for the horizontal and vertical seismic loads, q_H=q_V=1.0); medium subsoil class (i.e. subsoil class C, with subsoil parameters S_H=1.41 and S_V=1.00 in the horizontal and vertical directions, respectively); high-risk seismic zone (peak ground acceleration in the horizontal direction, PGA_H=0.283g, and peak ground acceleration in the vertical direction, PGA_V=0.201g). The gravity loads used in the design are represented by dead- and live loads, equal to: 4.4 kN/m^2 and 3 kN/m^2, for the top floor; 6.1 kN/m^2 and 3 kN/m^2, for the isolated floor; 5.7 kN/m^2 and 3 kN/m^2, for the other floors. The weight of the perimeter masonry infills, assumed as non-structural elements regularly distributed in elevation, is taken into account by considering a gravity load of 2.7 kN/m^2. A cylindrical compressive strength of 25 N/mm^2 for the concrete and a yield strength of 450 N/mm^2 for the steel are assumed for the r.c. frame members.

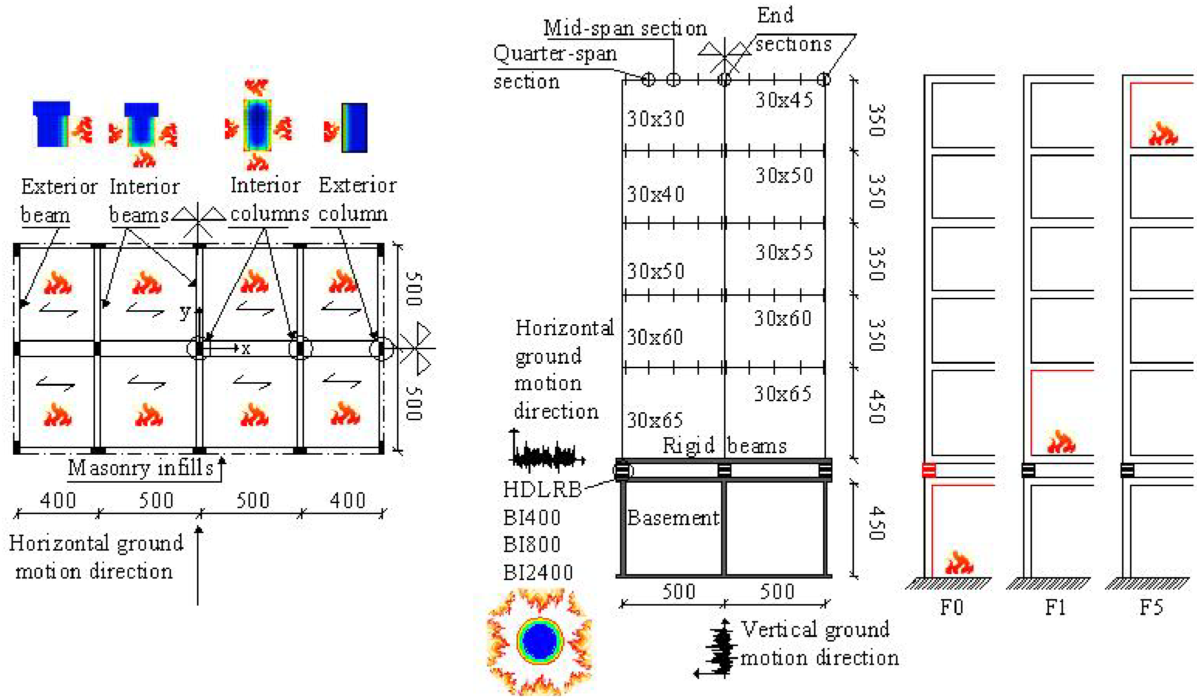

(a) Plan and fire compartment (b) Elevation and fire scenarios

Fig. 1 – Base-isolated test structure (units in cm)

Three test structures are considered, referring to a fundamental vibration period in the horizontal direction T_{1H}=2.5s and three vibration periods with prevailing component in the vertical direction: i.e. $T_{I,V}$=0.125s, 0.088s and 0.051s, for the BI400, BI800 and BI2400 structures, respectively. The design of the superstructure is carried out so as to satisfy minimum conditions for the longitudinal bars of the beams and columns, according to the provisions for low ductility class imposed by NTC08 [8]. The design of the HDLRBs fulfills the maximum shear strains: $\gamma_{tot}=\gamma_s+\gamma_c+\gamma_\alpha\leq 5$ and $\gamma_s\leq 2$, where γ_{tot} represents the total design shear strain, while γ_s, γ_c and γ_α represent the shear strains of the elastomer due to seismic displacement, axial compression and angular rotation, respectively. Moreover, the maximum compression axial load (P) does not exceed the critical load (P_{cr}) divided by a safety coefficient equal to 2.0. The minimum tensile stress (σ_{tu}) resulting from the seismic analysis is assumed as 2G(=0.7 MPa, for a shear modulus of the elastomer G=0.35 MPa).

In Table 1, depending on stiffness ratios α_{K0} considered in the analysis, the base isolation system properties are reported: i.e. the horizontal (K_{H0}) and vertical (K_{V0}) nominal stiffnesses and the corresponding equivalent damping coefficients (C_H and C_V), assuming an equivalent viscous damping ratio in the horizontal direction, ξ_H, equal to 10%, and an analogous ratio in the vertical direction, ξ_V, equal to 5%. The following geometrical and mechanical properties of the HDLRBs are also reported in Table 1: the diameter of the isolator (D); the total thickness of elastomer (t_e); primary (S_1) and secondary (S_2) shape factors; compression modulus (E_c). Finally, in Table 1 the results of the verifications for the HDLRBs are also reported. It is interesting to note that the design of the isolators depends on the condition imposed on the maximum values of γ_{tot} (i.e. BI800) and γ_s (i.e. BI2400) and minimum value of P_{cr}/P (i.e. BI400). In all the examined cases, no tensile forces are found in the isolators.

Table 1 – Properties and results of the verifications for the base-isolation system (units in kN and cm)

α_{K0}	K_{H0}	K_{V0}	C_H	C_V	D	t_e	S_1	S_2	E_c	γ_s	$\gamma_{tot,max}$	$(P_{cr}/P)_{min}$
400	81.80	32705	6.51	64.90	70.00	24.72	8.67	2.81	14.03	1.0	4.5	2.0
800	81.80	65409	6.51	91.80	59.20	17.67	12.80	3.35	28.00	1.4	5.0	2.3
2400	81.80	196227	6.51	159.00	48.78	12.00	30.15	4.06	84.00	2.0	4.8	3.9

Three fire scenarios with uniform temperature in the selected level are reported in Figs. 1a and 1b, assuming fire compartment is confined to the area of the base-isolated level (i.e. basement, F0) and the first (i.e. F1) and fifth (i.e. F5) levels of the superstructure. The Eurocode 1 (EC1) natural fire curve is used to simulate the time-temperature evolution during a fire [9], on the assumption that the fire load of the compartment is completely burnt out. In the heating phase, the gas temperature θ_g(°C)

$$\theta_g = 20 + 1325\left(1 - 0.324e^{-0.2t^*} - 0.204e^{-1.7t^*} - 0.472e^{-19t^*}\right) \tag{1}$$

is function of a fictitious time t^* obtained considering time t (in hours) multiplied by a dimensionless parameter equal to

$$\Gamma = \left(O/b\right)^2 / \left(0.04/1160\right)^2 \tag{2}$$

where b is the thermal absorptivity of surrounding surfaces of the compartment and O is an opening factor

$$O = A_v h_{eq}^{0.5} / A_t \tag{3}$$

depending on the total area of vertical openings (A_v), the weighted average of window heights (h_{eq}) and the total area of the compartment (A_t).

The gas temperature in the cooling phase is given by [9]

$$\theta_g = \theta_{max} - 250\left(3 - t^*_{max}\right)\left(t^* - t^*_{max}\right) \tag{4}$$

where the maximum temperature θ_{max} in the heating phase happens for

$$t^*_{max} = \left(0.2 \times 10^{-3} q_{t,d}/O\right)\Gamma \tag{5}$$

the design fire load density being

$$q_{t,d} = q_{f,d}\, A_f / A_t \tag{6}$$

related to the value $q_{f,d}$ corresponding to the surface area of the floor (A_f). With reference to 30 min (i.e. R30), 45 min (i.e. R45) and 60 min (i.e. R60) of exposure, the design parameters of the fire load are reported in Table 2 for the F1 and F5 fire scenarios in the superstructure. Further details on fire modelling can be found in [4].

Table 2 – Design parameters of fire curves for the F1 and F5 fire scenarios (units in MJ/m^2, $J/m^2s^{1/2}K$ and $m^{1/2}$)

	F1						F5					
	$q_{t,d}$	b	O_1	O_2	O_3	O_4	$q_{t,d}$	b	O_1	O_2	O_3	O_4
R30	127	1141					140	1142				
R45	175	1133	0.036	0.048	0.072	0.085	193	1134	0.026	0.040	0.053	0.079
R60	180	1132					198	1133				

EC1 time-temperature curves for different values of opening factor (O) and fire resistance (R) are shown in Figs. 2 and 3 considering the F1 and F5 fire scenarios for the superstructure, respectively. As can be observed, the maximum temperature in the heating phase generally increases with the ventilation but this trend is not evident for the temperatures corresponding to the fire resistance (i.e. R30, R45 and R60) because the total duration of the fire also decreases for increasing values of O.

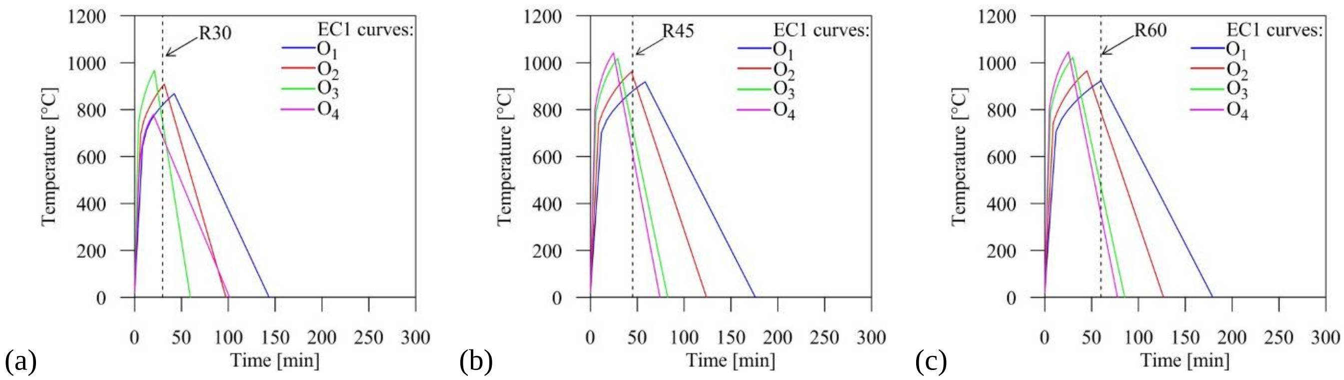

Fig. 2 – Natural (EC1) fire curves for different values of opening factor (O) and fire resistance (R): F1 fire scenario for the superstructure

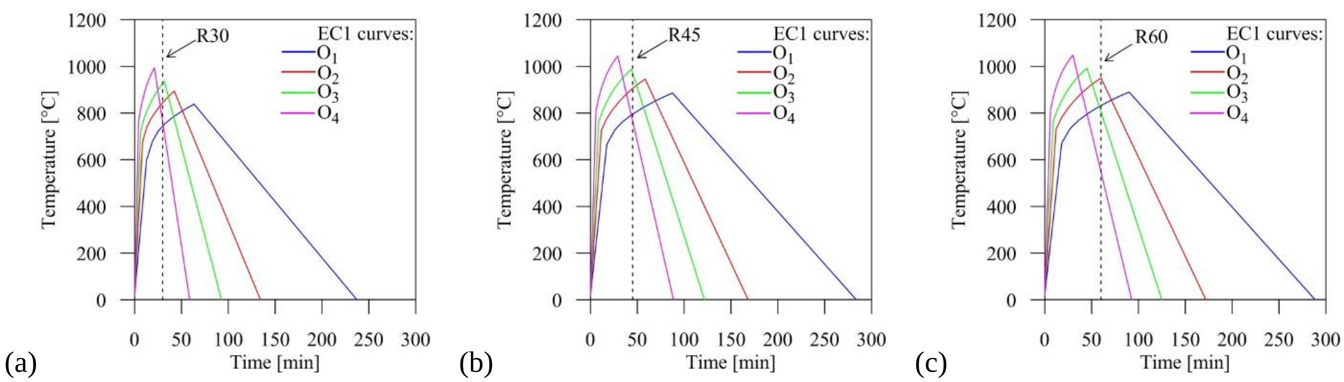

Fig. 3 – Natural (EC1) fire curves for different values of opening factor (O) and fire resistance (R): F5 fire scenario for the superstructure

Then, the fire-load design parameters in the basement (i.e. F0 fire scenario) are reported in Table 3, while the corresponding EC1 time-temperature curves are shown in Figs. 4a and 4b, assuming 15 min (i.e. R15) and 30 min (i.e. R30) of exposure to fire, respectively. Note that the opening factors (O_i, i=1-4) are selected so as to obtain the same temperature (i.e. 100 °C, 200 °C, 300 °C and 400°C) for both R15 and R30 fire resistances.

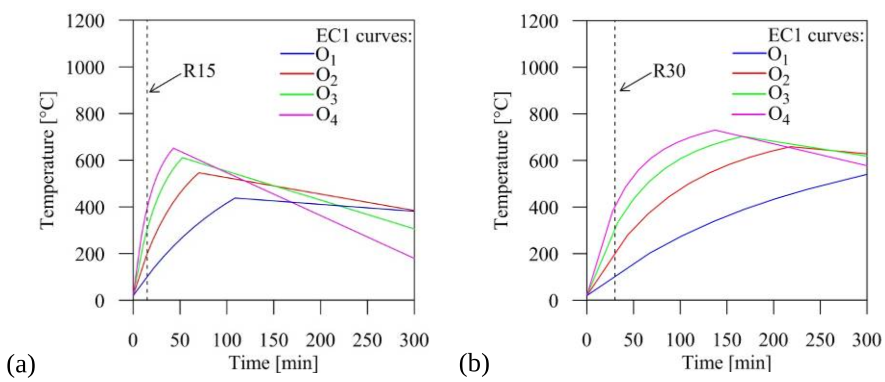

Fig. 4 – Natural (EC1) fire curves for different values of opening factor (O) and fire resistance (R): F0 fire scenario for the basement

Table 3 – Design parameters of fire curves for the F0 fire scenario (units in MJ/m^2, J/m^{2}s$^{1/2}$K and m$^{1/2}$)

	R15						R30					
	$q_{t,d}$	b	O_1	O_2	O_3	O_4	$q_{t,d}$	b	O_1	O_2	O_3	O_4
F0	58	1117	0.006	0.010	0.013	0.016	131	1099	0.005	0.007	0.009	0.011

3. Numerical results: fire loading

Once time-temperature curve of the fire compartment is determined with the EC1 model, it becomes possible to evaluate the temperature distribution in the r.c. frame members (Fig. 1a) and HDLRBs (Fig. 1b). Specifically, the thermal finite element cross-section model of columns, exposed to fire on one (exterior) and four (interior) sides, and beams, exposed to fire on one (exterior) and three (interior) sides, is considered assuming an ambient temperature of 20°C for the unexposed cross-section sides. Moreover, the thermal finite element cross-section model of HDLRBs exposed to fire on their lateral (cylindrical) surface is also considered.

The residual seismic load capacity of the r.c. cross-sections after fire is evaluated in line with the 500°C isotherm method of EC2 [10], in terms of reduction in stiffness, strength and ductility. The simplified calculation provides for a reduction of the cross-section size, with respect to a heat damaged zone defined by thermal mappings. In particular, concrete with temperatures exceeding 500°C, corresponding roughly to the thickness of the unconfined zone, is assumed not to contribute, while the residual concrete cross-section retains its initial values of strength and modulus of elasticity. On the other hand, a reduced yield strength of each longitudinal reinforcement bar, in the tension and compression zones of the cross-section, is evaluated on the basis of the steel temperature profile in the centre of the bar.

In Fig. 5 ultimate strength and ductility in the r.c. cross-section of the interior columns are reported at the end of 60 (i.e. F.R60 structure) minutes of exposure to fire, considering different values of the opening factor (i.e. O_i, i=1-4).

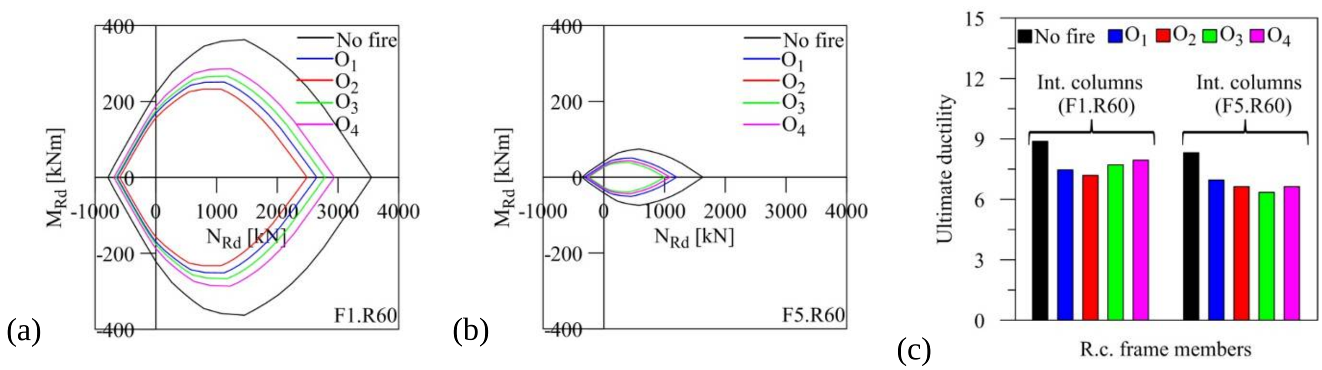

Fig. 5 – Ultimate strength and ductility of r.c. interior columns exposed to fire

In detail, the ultimate interaction domain between axial load (N_{Rd}) and bending moment (M_{Rd}) are examined for fire scenario at the first (i.e. F1 in Fig. 5a) and fifth (i.e. F5 in Fig. 5b) level, assuming the direct correspondence between the examined level and the fire compartment. Note that interior columns exhibit a marked narrowing of their N_{Rd}-M_{Rd} domains, especially for compressive axial load greater than that of the balanced compressive load. For this axial load, a local reduction in flexural strength, in comparison with the no-fire condition, of about 21% and 36%, at the first storey, and 32% and 47%, at the fifth storey, is found for the extreme values of the opening factor. On the other hand, limited effects of the opening factor are observed on the ultimate ductility (Fig. 5c) with a global mean decrease of about 15% (F1.R60 structure) and 20% (F5.R60 structure) in comparison with the no-fire condition. Further results, which are omitted for the sake of brevity, have confirmed limited fire effects in the exterior columns.

In Fig. 6, similar graphs show ultimate strength and ductility in the top- and bottom-side of fire-exposed cross-sections of interior beams. Specifically, the end, quarter- and mid-span sections of the F1.R60 (Figs. 6a-6c) and F5.R60 (Figs. 6d-6f) structures are compared with the no fire condition. A significant decrease in strength is observed on the bottom-side of all sections, with a global mean reduction of about 18% and 32%, at the first storey (Fig. 6a), and 15% and 34%, at the fifth storey (Fig. 6d), for the extreme values of the opening factor. Note that a mean increase of ductility of about 5% and 2% is obtained on the bottom-side of the F1.R60 (Fig. 6b) and F5.R60 (Fig. 6e) structures, respectively, due to the fire-reduced yield strength of the longitudinal bars in tension. On the other hand, mean value of ultimate ductility at the top-side decreases by about 11% (i.e. F1.R60 in Fig. 6c) and 15% (i.e. F5.R60 in Fig. 6f), respectively. This behaviour occurs because of heat damage to the compression zone of concrete and corresponding longitudinal reinforcement. Negligible effects, omitted for the sake brevity, are obtained for the exterior beams. As reported in previous works [4, 5], a significant decrease in flexural stiffness is found in the structural members exposed to fire.

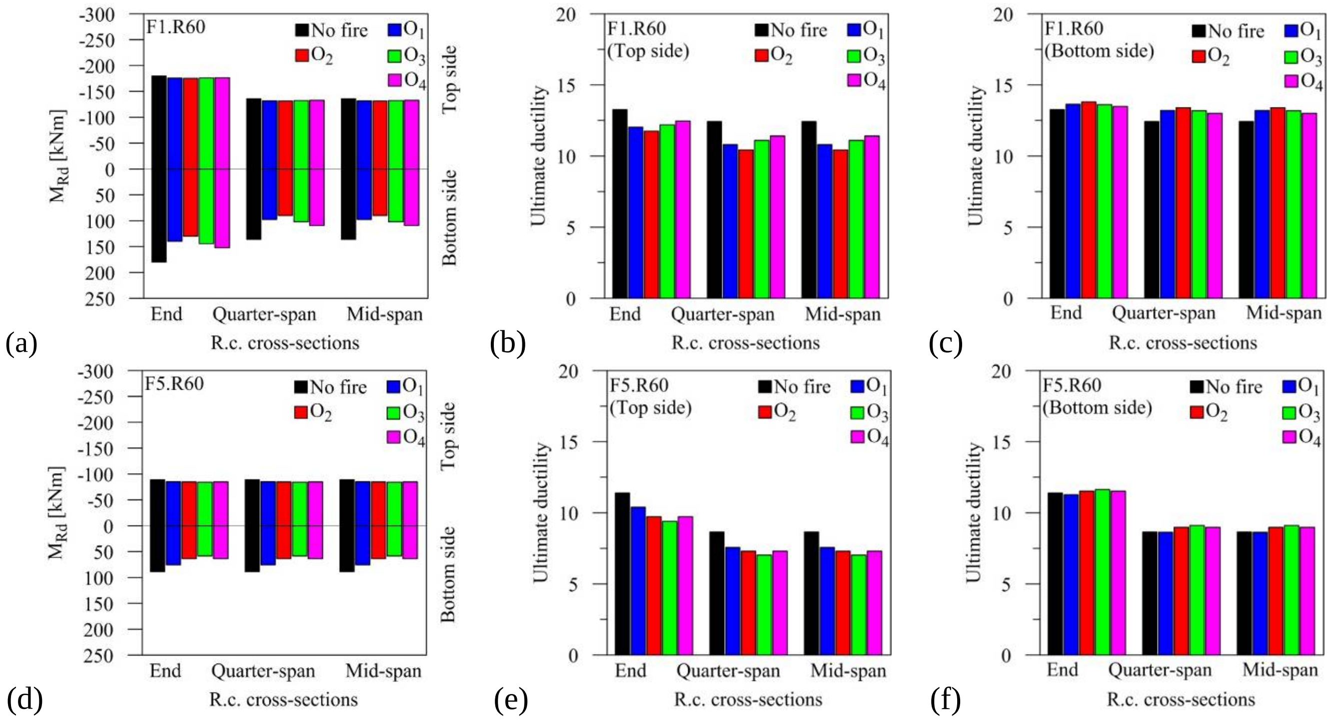

Fig. 6 – Ultimate strength and ductility of r.c. interior beams exposed to fire

The residual seismic load capacity following fire of the HDLRBs is evaluated in line with a proposed 200°C isotherm method, in which rubber with temperatures exceeding 200°C, corresponding roughly to the vulcanization temperature between layers of rubber and steel plates [8], is assumed not to contribute, while the residual cross-section retains its initial values of strength and stiffness. The question of predicting the inner radius (R_2) of the steel plates of the HDLRB where the temperature T_2=200°C is reached, assuming the outer radius (R_1=D/2, where D is the original diameter of the isolator) and temperature ($T_1=T_{Fire}$) as known boundary quantities, is formulated as a heat conduction problem in an infinite circular cylinder

$$Q_s = 2\pi k_s t_s \frac{T_1 - T_2}{\ln(R_1/R_2)} \tag{7}$$

being k_s (i.e. 15 W/(m°C)) the thermal conductivity of the steel and t_s the total plates thickness of the HDLRB. In terms of infinite integral of Bessel, a solution to this problem is proposed in [13]

$$T^+ = k_s T_1/(q_s R_1) \tag{8}$$

but a good approximation of the dimensionless temperature T^+ is also given by [7]

$$T^+ = 0.785(t^+)^{1/3} \tag{9}$$

as function of the dimensionless time

$$t^{+} = d_s t / R_1^2 \tag{10}$$

where d_s is the thermal diffusivity (i.e. 1.41×10^{-5} m^2/s) of the steel. With some manipulation, Eq. (8) and Eq. (9) lead to the following expression of heat flowing per unit surface due to the fire exposure

$$q_s = k_s T_1 \Big/ \left[0.785 R_1 (t^{+})^{1/3} \right] \tag{11}$$

corresponding to the total heat flowing

$$Q_s = 2\pi R_1 t_s q_s \tag{12}$$

For instance, temperature profiles of the HDLRBs are plotted in Fig. 7 at the end of 30 minutes (i.e. R30) of exposure, assuming an ambient temperature of 20 °C for the inner part of the isolator. As can be observed, the isotherm T_2=200 °C is reached more quickly for decreasing values of the initial radius of curvature (R_1) of the isolators: e.g., with reference to the fire temperature T_1=400 °C, corresponding to the opening factor O_4 (see Table 3), a decrease of R_1 of about 21%, 23% and 26% is obtained for the BI400 (Fig. 7a), BI800 (Fig. 7b) and BI2400 (Fig. 7c) structures, respectively.

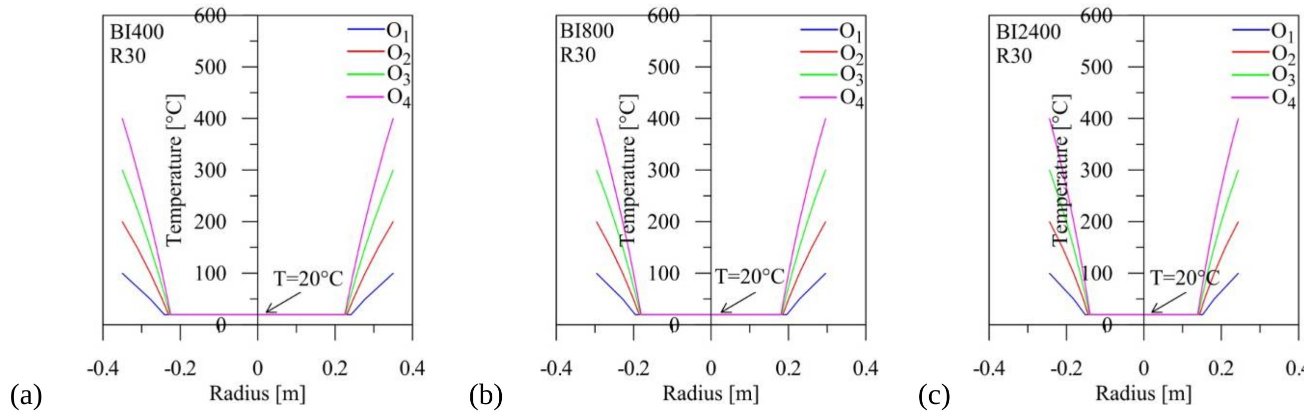

Fig. 7 – Temperature profiles of HDLRBs exposed to fire

Next, reduction factors of mechanical and geometrical properties of the HDLRBs are plotted in Fig. 8, at the end of 15 (i.e. R15) and 30 (i.e. R30) minutes of exposure, with fire temperatures in the basement increased up to 600°C. More specifically, reduction factors for the horizontal (i.e. $\alpha_{KH,T}$=$K_{H,T}$/K_{H0}) and vertical (i.e. $\alpha_{KV,T}$=$K_{V,T}$/K_{V0}) stiffnesses and the primary and secondary shape factors (i.e. $\alpha_{S,T}$=$S_{1,T}$/S_1=$S_{2,T}$/S_2) are reported, assuming three values of the nominal stiffness ratio (i.e. α_{K0}=400, 800 and 2400). It is interesting to note that the highest reduction factors are obtained for the vertical stiffness (Fig. 8a) followed by the horizontal one (Fig. 8b), while the shape factors are less sensitive to fire loads (Fig. 8c).

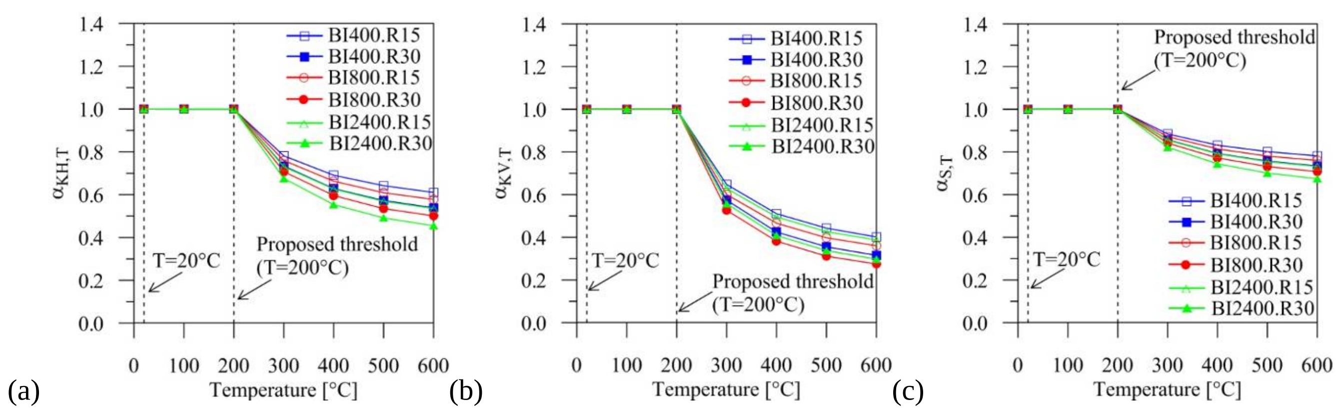

Fig. 8 – Reduction factors of mechanical and geometrical properties of HDLRBs exposed to fire

4. Numerical results: seismic loading

A numerical investigation is carried out to study the nonlinear seismic response of the base-isolated r.c. framed buildings damaged by the fire loading, at different durations of fire resistance for the superstructure (i.e. R30, R45 and R60) and the basement (i.e. R15 and R30), and subjected to near-fault ground motions. Three earthquakes (EQs), each recorded at three stations, are selected from the Pacific Earthquake Engineering Research center database [11]. For each motion, time-histories of the horizontal components of acceleration are first projected along the direction of the strongest observed pulse [12]. Long-duration horizontal pulses due to forward-directivity and fling-step effects characterize Chi-Chi (Taiwan, 1999) and Northridge (California, 1994) earthquakes, respectively, while high values of the peak acceleration ratio α_{PGA}(=PGA_V /PGA_H), defined as the ratio between the peak value of the vertical acceleration (PGA_V) and the corresponding value of the horizontal acceleration (PGA_H), are evident in the Imperial Valley (California, 1979) earthquake. The main data of the selected EQs are shown in Table 4: i.e. earthquake, year, recording station, magnitude (M_w), closest distance to the fault (Δ), horizontal (PGA_{H1} and PGA_{H2}) and vertical (PGA_V) peak ground accelerations, maximum value of the acceleration ratio ($\alpha_{PGA,max}$); orientation in degrees clockwise from North of the strongest observed pulse (ϕ).

The r.c. frame members are idealized by means of a two-component model, constituted of an elastic-plastic component and an elastic component, assuming a bilinear moment-curvature law [4, 5]. Plastic conditions are assessed at the potential critical sections of the beams (i.e. end sections of the sub-elements in which a beam is discretized) and columns (i.e. end sections), where reduced value of stiffness, strength and ductility properties are assumed at the levels where the fire compartment is confined (i.e. F1 and F5 fire scenarios). The effect of the axial load on the ultimate bending moment of the columns (M-N interaction) is also considered. The response of the HDLRBs is simulated with a viscoelastic model with variable stiffness properties in the horizontal and vertical directions, depending on the axial force and lateral deformation [1]. Mechanical and geometrical properties of the HDLRBs are reduced when fire temperatures exceed 200°C, assuming F0 fire scenario (i.e. fire compartment at the basement). Incremental dynamic analysis (IDA) of the test structures is carried out by using a series of nonlinear dynamic analyses, scaling each horizontal and vertical motion to a submultiple (a_g) of the corresponding PGA value reported in Table 4. Afterwards, the maximum of the results separately obtained for these EQs is calculated. It should be noted that nonlinear IDAs under the selected near-fault EQs are terminated once a limit state is reached: i.e. ultimate ductility demand at the critical sections of beams and columns; ultimate total shear strain ($\gamma_{tot,u}$) and corresponding shear strain due to seismic displacement ($\gamma_{s,u}$) of the HDLRBs, which are assumed equal to 1.5 times the design values; maximum compression axial load (P), which does not exceed the critical load (P_{cr}), and tensile axial load, obtained by multiplying the reduced effective area by a limit stress tension equal to 0.7 MPa, of the HDLRBs

Table 4 – Main data of the selected near-fault ground motions

Earthquake	Recording station	M_w	Δ	PGA_{H1}	PGA_{H2}	PGA_V	$\alpha_{PGA,max}$	ϕ
Chi-Chi, 1999	TCU051	7.6	7.6 km	0.16g	0.24g	0.11g	0.69	100°
	TCU059	7.6	17.1 km	0.16g	0.17g	0.07g	0.44	45°
	TCU065	7.6	0.6 km	0.79g	0.58g	0.26g	0.45	113°
Imperial Valley, 1979	El Centro D.A.	6.5	5.1 km	0.35g	0.48g	0.77g	2.20	253°
	El Centro Array #7	6.5	0.6 km	0.34g	0.47g	0.58g	1.71	56°
	El Centro Array #5	6.5	4.0 km	0.53g	0.38g	0.59g	1.55	228°
Northridge, 1994	Rinaldi	6.7	6.5 km	0.87g	0.47g	0.96g	2.04	209°
	Newhall Fire Station	6.7	5.9 km	0.58g	0.59g	0.55g	0.95	21°
	Newhall W P.C.	6.7	5.5 km	0.42g	0.36g	0.30g	0.83	34°

First, maximum global ductility demand of base-isolated structures at the end of 60 (i.e. R60) minutes of fire exposure is plotted in Fig. 9, on the assumption that the fire compartment is confined to the area of: the first level (i.e. F1 scenario, Figs. 9a,d), under Chi-Chi EQs; the fifth level (i.e. F5 scenario, Figs. 9b,e), under Imperial Valley EQs; the first (i.e. F1 scenario, Fig. 9c) and fifth (i.e. F5 scenario, Fig. 9f) levels, under Northridge EQs. Two values of the nominal stiffness ratio (α_{K0}) of the HDLRBs, corresponding to the BI400 and BI2400 structures, are examined in the no fire condition and in the case of fire with different levels of ventilation (i.e. O_i, i=1-4). As can be observed, an amplification in the structural response of fire-exposed base-isolated structures is generally obtained for increasing values of the dimensionless acceleration $\alpha_a(=a_g/PGA)$. In detail, the IDAs are interrupted once the ultimate value imposed on the maximum ductility demand is reached for the interior beams: at the bottom-side of quarter-span sections of the first level, under the Chi-Chi EQ (TCU065 station), for both BI400 and BI2400 structures, and the Imperial Valley (El Centro A#5 station) and Northridge (Newhall W P.C. station) EQs, for the BI400 structures; at the bottom side of mid-span sections of the fifth level, under the Imperial Valley (El Centro A.#5 station) and Northridge (Rinaldi station) EQs, for BI2400 structures. A significant variation of ductility demand is highlighted assuming different values of the opening factor, with the exception of the F5 fire scenario for BI400 structures subjected to Imperial Valley EQs (Fig. 9b). This can be explained by the fact that for $\alpha_{K0}\rightarrow 0$ the structure above the isolation system can be considered isolated in the vertical direction and failure occurs at the lower levels, which are not influenced by fire.

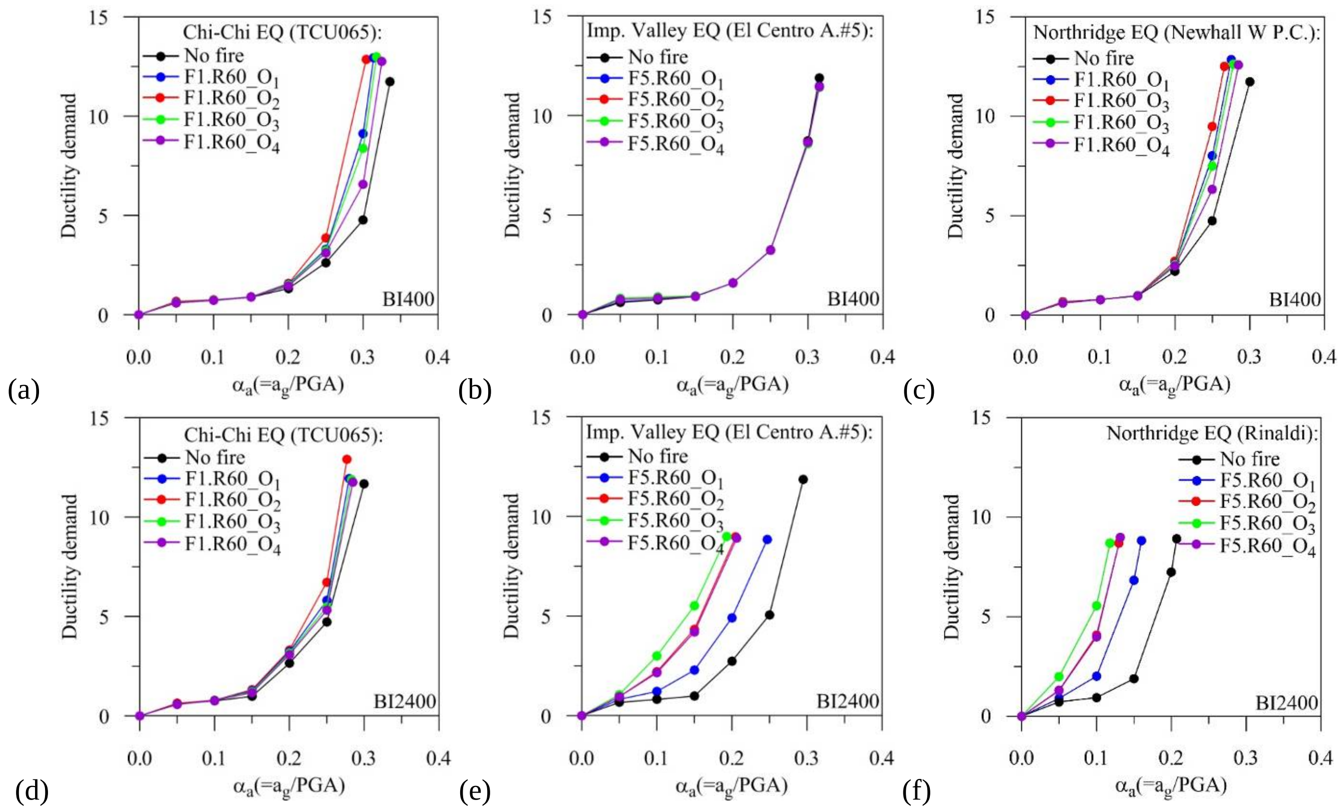

Fig. 9 – Global ductility demand of r.c. interior beams for different fire scenarios in the superstructure

Afterwards, maximum values of the P/P_{cr} ratio and total shear strain (γ_{tot}) for the interior (central) HDLRB in the basement are plotted in Fig. 10, at the end of 30 (i.e. R30) minutes of fire exposure. More specifically, the most detrimental opening factors (i.e. O_3 and O_4 in Table 3, corresponding to the fire temperatures T=300°C and 400°C, respectively) are considered for the BI400, BI800 and BI2400 structures subjected to the Chi-Chi (Figs. 10a,d), Imperial Valley (Figs. 10b,e) and Northridge (Figs. 10c,f) EQs. Indeed seismic response of the base-isolation system is strongly affected by the amount of ventilation during fire: for each value of α_{K0}, the IDAs are interrupted for wide ranges of α_a when different opening factors are considered. Moreover, the buckling failure occurs sooner for lower values of α_{K0} (e.g. BI400 and BI800 structures) than for higher ones (e.g. BI2400 structure), when high values of the opening factor (e.g. O_4) are considered (Figs. 10a-

10c). On the other hand, the BI800 and BI2400 structures generally collapse before the BI400 structure, because the limit value imposed on γ_{tot} is exceeded when lower values of the opening factor (e.g. O_3) are assumed (Figs. 10d-10e). The only exception is the BI2400_O_3 structure subjected to the Northridge EQ (Figs. 10c,f), where the ultimate tensile axial load is attained.

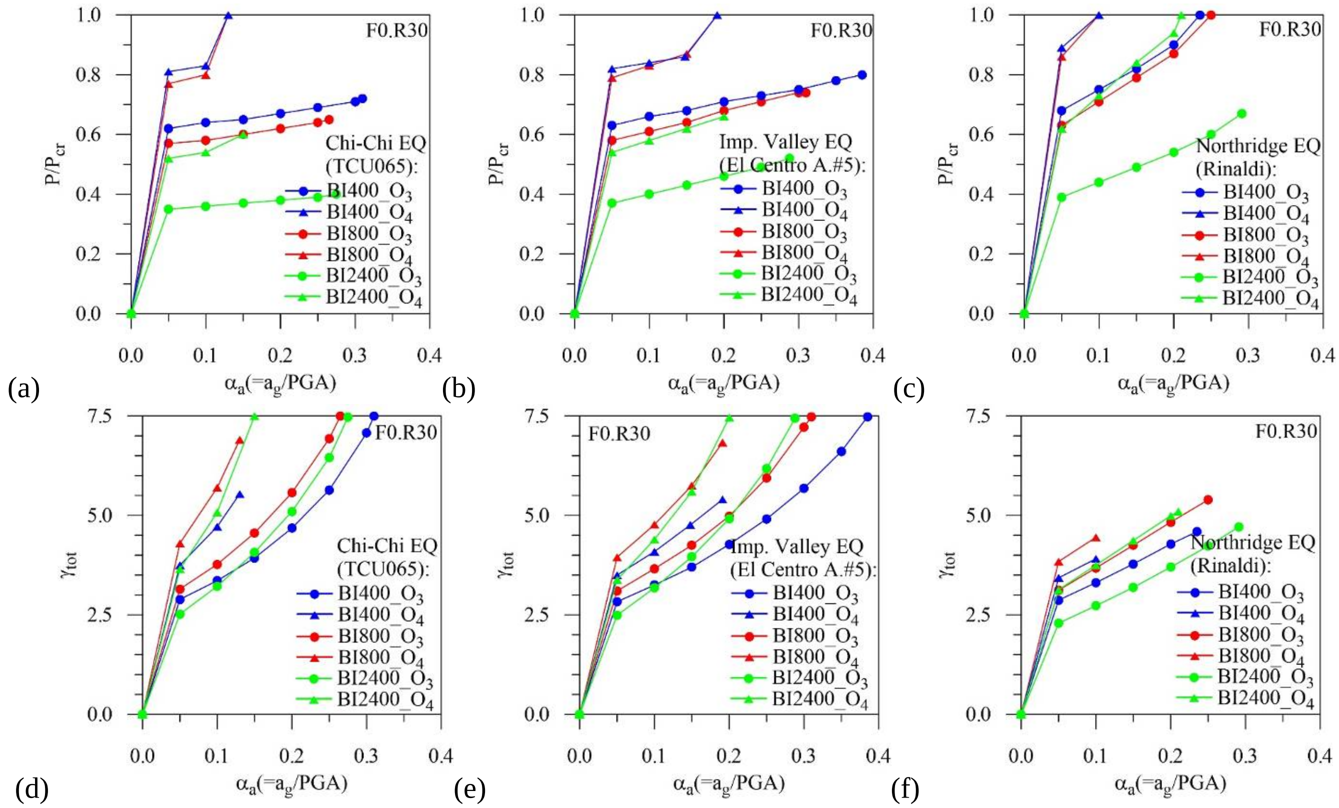

Fig. 10 – Axial load and total shear strain of central HDLRBs for different fire scenarios in the basement

Finally, curves similar to the previous ones are reported in Fig. 11 to compare the seismic response of the F0.R30, F1.R60 and F5.R60 structures with the no-fire condition. As can be observed, the pulse-type nature of the horizontal component of the Chi-Chi EQs can induce unexpected ductility demand especially at the lower levels (see comments to Figs. 9a,d), with an amplification when the fire compartment at these levels and R60 are assumed, which can be less dangerous than fire in the basement, where collapse of the HDLRBs is expected (Fig. 11a). On the other hand, the amplification in the ductility demand highlighted at the upper levels of fire-exposed base-isolated structures (see comments to Figs. 9b,c,e,f) is comparable, in terms of maximum acceleration ratio α_a, with fire damage of the HDLRBs at the basement, when the Imperial Valley and Northridge EQs are considered (Figs. 11b,c).

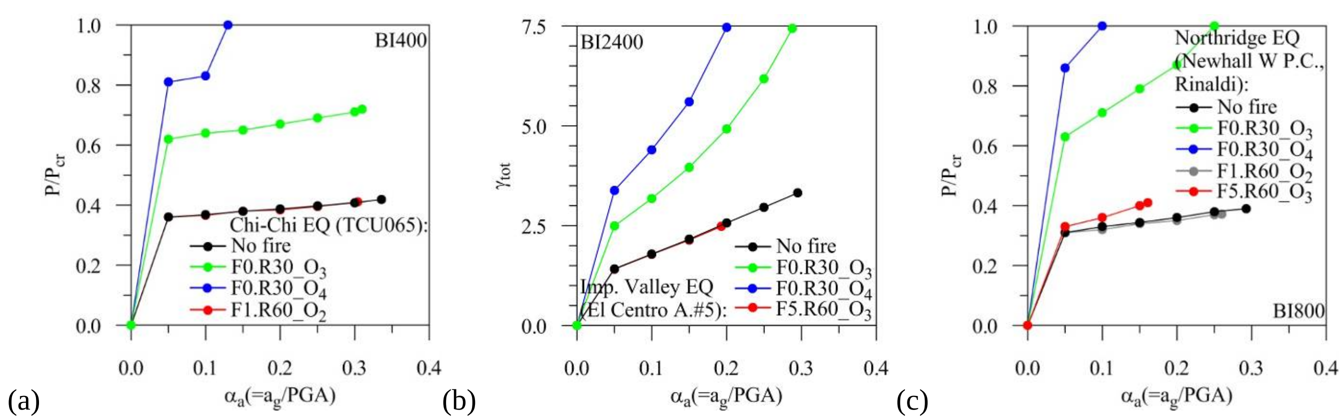

Fig. 11 – Axial load and total shear strain of central HDLRBs

for different fire scenarios in the superstructure and basement

5. Conclusions

To study the nonlinear dynamic response following fire of base-isolated structures with HDLRBs subjected to near-fault earthquakes, a numerical investigation is carried out on r.c. six-storey framed buildings composed of a basement and five storeys above the isolation level. Three fire scenarios are considered, assuming the fire compartment confined to the area of the base-isolated level (i.e. F0) and first (i.e. F1) and fifth (i.e. F5) levels of the superstructure. The residual seismic load capacity of the fire-exposed HDLRBs is evaluated in line with a proposed 200°C isotherm method, in which rubber with temperatures exceeding this value is neglected. The highest reduction factors are obtained for the vertical stiffness of the HDLRBs followed by the horizontal one, while primary and secondary shape factors are less sensitive to fire loads. Then, the nonlinear incremental dynamic analysis of base-isolated structures in a no fire situation is compared with that in the event of fire, considering three near-fault earthquakes each recorded at three stations. A significant variation of ductility demand, in r.c. frame members, and axial load and total shear strain, in HDLRBs, are highlighted assuming different values of the opening factor during fire. The pulse-type nature of the horizontal component of the Chi-Chi EQs can induce unexpected ductility demand especially at the lower levels, which can be less dangerous than fire in the basement where collapse of the HDLRBs is expected. On the other hand, the amplification in the ductility demand highlighted at the upper levels of fire-exposed base-isolated structures is comparable, in terms of maximum acceleration ratio α_a, with fire damage of the HDLRBs in the basement when the Imperial Valley and Northridge EQs are considered.

6. Acknowledgements

The present work was also financed by Re.L.U.I.S. (Italian network of university laboratories of earthquake engineering), in accordance with “Convenzione D.P.C.–Re.L.U.I.S. 2014–2016, WPI, Isolation and Dissipation”.

7. References

[1] Mazza F, Vulcano A (2012): Effects of the near-fault ground motions on the nonlinear dynamic response of base-isolated r.c. framed buildings. *Earthquake Engineering and Structural Dynamics*, **41**(2), 211-232.

[2] Bray JD, Rodriguez-Marek A, Gillie JL (2009): Design ground motions near active faults. *Bulletin of the New Zealand Society for Earthquake Engineering*, **42** (1), 1-8.

[3] Elgamal A, He L (2004): Vertical earthquake ground motion records: An overview. *Journal of Earthquake Engineering*, **8** (5), 663-697.

[4] Mazza F, (2015): Seismic vulnerability and retrofitting by damped braces of fire-damaged r.c. framed buildings. *Engineering Structures*, **101** (10), 179-192.

[5] Mazza F, Alesina F (2016): Effects of site condition in near-fault area on the nonlinear response of fire-damaged base-isolated structures. *Engineering Structures*, **111** (3), 297-311.

[6] Bhowmick AK, Mukhopadhyah R, De SK (1979): High temperature vulcanization of elastomers. *Rubber Chemistry and Technology*, **52** (4), 725-734.

[7] Kalpakidis IV, Constantinou MC (2009): Effects of heating on the behavior of lead-rubber bearings. I: Theory. *Journal of Structural Engineering*, **135** (12), 1440-1449.

[8] NTC08 (2008): Technical Regulations for the Constructions. Italian Ministry of the Infrastructures (in Italian).

[9] Eurocode 1 (2004): Actions on structures – Part 1-2: General actions, actions on structures exposed to fire. C.E.N., European Committee for Standardization.

[10] Eurocode 2 (2004): Design of concrete structures – Part 1-2: General rules, structural fire design. C.E.N., European Committee for Standardization.

[11] Pacific Earthquake Engineering Research Center database. http://ngawest2.berkeley.edu.

[12] Pulse Classifications from NGA West2 database 2012. http://web.stanford.edu/~bakerjw/pulse_classification_v2/Pulse-like-records.html

[13] Carslaw HS, Jaeger JC (1959): *Conduction of Heat in Solids*. Oxford University (U.K.), 2nd edition.